Sustainable Cities and Society 101 (2024) 105084

Contents lists available at ScienceDirect

Sustainable Cities and Society

journal homepage: www.elsevier.com/locate/scs

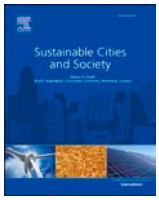

Climate change impacts assessment on railway infrastructure in urban environments

Ahmad Kasraei [a,*], A.H.S. Garmabaki [a], Johan Odelius [a], Stephen M Famurewa [a,b], Khosro Soleimani Chamkhorami [a,d], Gustav Strandberg [c]

[a] Department of Civil, Environmental, and Natural Resources Engineering, Division of Operation, Maintenance and Acoustics, Luleå University of Technology, Luleå, 97187, Sweden
[b] Swedish Transport Administration, Luleå, Sweden
[c] Rossby Centre, Swedish Meteorological and Hydrological Institute, SMHI, Sweden
[d] Department of Mathematics, Faculty of Computer Engineering, Najafabad Branch, Islamic Azad University, Najafabad, Iran

ARTICLE INFO

Keywords:
Climate change adaptation
Reliability analysis
Cox proportional hazard model
Railway infrastructure

ABSTRACT

Climate change impacts can escalate the deteriorating rate of infrastructures and impact the infrastructure's functionality, safety, operation and maintenance (O&M). This research explores climate change's influence on urban railway infrastructure. Given the geographical diversity of Sweden, the railway network is divided into different climate zones utilizing the K-means algorithm. Reliability analysis using the Cox Proportional Hazard Model is proposed to integrate meteorological parameters and operational factors to predict the degree of impacts of different climatic parameters on railway infrastructure assets. The proposed methodology is validated by selecting a number of switches and crossings (S&Cs), which are critical components in railways for changing the route, located in different urban railway stations across various climate zones in Sweden. The study explores various databases and proposes a climatic feature to identify climate-related risks of S&C assets. Furthermore, different meteorological covariates are analyzed to understand better the dependency between asset health and meteorological parameters. Infrastructure asset managers can tailor suitable climate adaptation measures based on geographical location, asset age, and other life cycle parameters by identifying vulnerable assets and determining significant covariates. Sensitivity analysis of significant covariates at one of the urban railway stations shows precipitation increment reveal considerable variation in the asset reliability.

1. Introduction

To understand the behavior of the railway system, it is essential to consider various operational factors that influence railway network performance (Barabadi Abbas et al., 2011; Gao et al., 2010). Climate change poses multiple challenges to the O&M of railway infrastructures. The projected changes in climate, including alterations in precipitation patterns, temperature variations, severe snowfall, and sea level rise, are examples of these extra pressures on the functioning of railway infrastructure assets. These climatic consequences may lead to reducing availability, safety, punctuality performance indices, and increased O&M costs (Garmabaki et al., 2022; Garmabaki et al., 2021; IPCC., 2022; Miller & Huntsinger, 2023; Pour et al., 2020; Salimi & Al-Ghamdi, 2020; Thaduri et al., 2021).

According to Forzieri et al. (2018), transport infrastructure in Europe faces potential climate risks, such as heatwaves, cold waves, droughts, wildfires, river and coastal floods, and windstorms. These risks may escalate from €0.5 billion to more than €10 billion by the 2080s. For instance, the winter temperature is expected to rise above the annual average temperature, with the most significant increase in northern Sweden. It may be noted that the extent of infrastructure damage may vary depending on the design, age, and operational conditions of specific infrastructure, considering local geological and ecological requirements.

In addition to the extreme impacts of flooding and heatwaves, the frequent occurrence of flood events exacerbates disruptions in railway operations, resulting in speed restrictions, blockages, discomfort for passengers, and interruptions in the supply chain. Heatwaves could

* Corresponding author at: Division of Operation, Maintenance and Acoustics, Department of Civil, Environmental, and Natural Resources Engineering, Luleå University of Technology, SE-97187, Sweden.
E-mail address: Ahmad.kasraei@associated.ltu.se (A. Kasraei).

https://doi.org/10.1016/j.scs.2023.105084
Received 24 August 2023; Received in revised form 24 October 2023; Accepted 24 November 2023
Available online 25 November 2023

triple the speed restrictions on railways in certain parts of the UK to minimize the risk of track buckling (Ferranti et al., 2018; Palin et al., 2013; Vogel et al., 2019). In Eastern Europe (EEU) and northern Scandinavia, the increased number of freezing-thawing cycles experienced by construction materials amplifies the infrastructure's failure rate and associated risks (Nilsen et al., 2021; Yakubovich & Yakubovich, 2018).

As a result of global warming Western Central Europe (WCE) and Northern Europe (NEU) will experience a higher frequency of extreme hourly precipitation events during summer. For example, projections indicate that beyond a Global Warming Level (GWL) of 3 °C, Germany and the UK may experience a two- or tenfold increase, respectively, for events exceeding the present-day 99.99th percentile (IPCC., 2022). In autumn and winter, these increases are expected to extend more widely across Europe, with Southern Europe (SEU) experiencing a higher than tenfold rise in 99.99th percentile events (Chan Steven et al., 2020). Moreover, beyond a GWL of 2 °C, landslide risks in WCE and SEU may increase, posing further threats to transport networks (Guido Rianna et al., 2020; Rianna et al.; Schlögl & Matulla, 2018).

At a GWL of 1.5–3 °C, the existing flood risk for railways, particularly in WCE, is projected to increase twofold or even triple. This heightened flood risk carries significant financial implications, with rail transport in Europe requiring an additional expenditure of 1.22 billion EUR annually under a 3 °C GWL scenario without any adaptation measures in place (Bubeck Philip et al., 2019). Furthermore, the anticipated rise in thermal discomfort within urban underground railways is expected, even with substantial carriage cooling measures in place (Jenkins et al., 2014).

Reliability and resilience analysis are two important performance measures for infrastructure asset managers while aiming to assess climate change impacts. There are various approaches available for analyzing the reliability and maintainability performance of the assets, including qualitative methods such as failure modes, effects, and criticality analysis (FMECA), fault tree analysis (FTA), event tree analysis (ETA), reliability block diagrams (RBDs), reliability centered maintenance (RCM), and Bayesian networks (BNs) (Kumar & Banerji, 2022; Rausand, 2020). On the other hand, quantitative approaches enable the analysis of the effects of explanatory variables/covariates on reliability, such as the accelerated failure time (AFT) model, the Arrhenius model, and the proportional hazard model (PHM) (Rausand, 2020).

As a flexible model, PHM was successfully used to assess the impact of different covariates, such as operational conditions on the reliability and maintenance assessment. The model can also effectively account for the effects of various factors on the time-to-failure of components, such as operating conditions, maintenance actions, and design characteristics. For instance, the study by Thijssens and Verhagen (2020) evaluates the use of an extended Cox PHM in analyzing time-on-wing data of aircraft components, finding that it provides a more accurate prediction of time-to-failure than traditional survival analysis methods.

In another study, Barabadi Abbas et al. (2014); Ghodrati (2005) used the PHM to predict and optimize spare parts planning. The PHM was used to model the failure rate of spare parts based on covariates such as operating hours and usage history. Liu et al. (2020) used PHM to develop a maintenance strategy considering system components' aging and cumulative damage. The authors showed that this approach can effectively predict maintenance needs and improve system reliability through simulations and case studies. Chen Chong et al. (2020) have combined the Cox PHM with deep learning (DL) techniques called Cox proportional hazards deep learning (CoxPHDL) to improve the accuracy of maintenance predictions. Zheng et al. (2021) proposed a PHM incorporating degradation trends and environmental factors to predict product reliability. The research suggests that considering degradation trends and environmental factors can improve the accuracy of reliability predictions and provide helpful information for product reliability management.

This paper aims to integrate the impact of meteorological factors such as temperature, precipitation, wind speed, and relative humidity with railway infrastructure asset health conditions. The goal is to analyze how climate change affects the behavior of urban railway infrastructure assets. To achieve this goal, an unsupervised machine learning algorithm is applied to categorize the Swedish railway network into different climate zones, including diverse urban railway assets from various regions. The study assesses the influence of climatic factors on the reliability of urban railway assets using the Cox proportional hazards model (Cox PHM). Additionally, a sensitivity analysis is conducted to estimate the effect of variations in weather parameters on the performance of these assets.

The rest of the paper is as follows: Section 2 addresses meteorological parameters and their impacts on railway infrastructure, future climatic scenarios, and climate change adaptation strategies. Section 3 describes the proposed methodology in five phases. Section 4 presents the case study and obtained results. The paper is concluded by summarizing the key findings in Section 5.

2. Preliminary study

This section provides some insightful perspectives regarding the effect of weather parameters on the infrastructure's failures. In addition, it describes how future climate scenarios can affect the weather conditions globally and in Sweden. Moreover, it provides different climate adaptation strategies to mitigate climate impacts.

2.1. Relationship between climatic conditions and asset failures

Climate impact assessment can be categorized into two general groups as: macroscopic and microscopic approaches. The short description of each category is as follows:

2.1.1. Macroscopic climatic impact assessment

In this approach, a certain zone/ predefined geographical area will be considered without taking into account the specific asset and its associated failure behavior. The size of geographical location can be defined utilizing different features, for instance, maintenance areas, cities, provinces, etc. Therefore, all the failure modes in this zone will be integrated and analyzed together. In this approach, climate parameters will be considered at lower resolution by integrating various weather stations parameters, for instance, average temperature as an indicator for the whole province. This approach can be effective for vulnerability and risk assessment of specific climate impact over the railway network, for instance, identification of vulnerable areas/assets to the flooding in a vast area. Fig. 1 shows the projected precipitation and temperature for the period 2071–2100 based on an average of 17 combinations of global and regional climate models for emissions scenario RCP8.5 (this concept is discussed in Section 2.2) for Sweden. These maps enable infrastructure asset managers to formulate strategic plans for O&M of the railway network that may be vulnerable to climatic hazards like flooding or track buckling.

2.1.2. Microscopic climatic impact assessment

Due to heterogeneity in asset types, utilizing a macroscopic approach may raise some modelling inconsistencies since various infrastructure asset types have been installed within the Swedish railway network. In the microscopic approach, climate parameters will be considered at a higher resolution, and a homogeneous group of assets will be considered for the assessment. Therefore, all the features, including failure causes, failure modes, geographical locations, local weather parameters at the asset level will be collected for the climatic impact assessment.

This paper has followed the microscopic approach for climatic impact assessment. To assess the impact of climate parameters on asset health, there is a need to identify failure causes due to climatic reasons at the asset level. Climate_id indicator has been designed based on climate parameters to classify asset failures into climatic and non-climatic causes, which will be discussed in Section 3.1.

Fig. 2 shows the number of assets' failures classified as climatic and

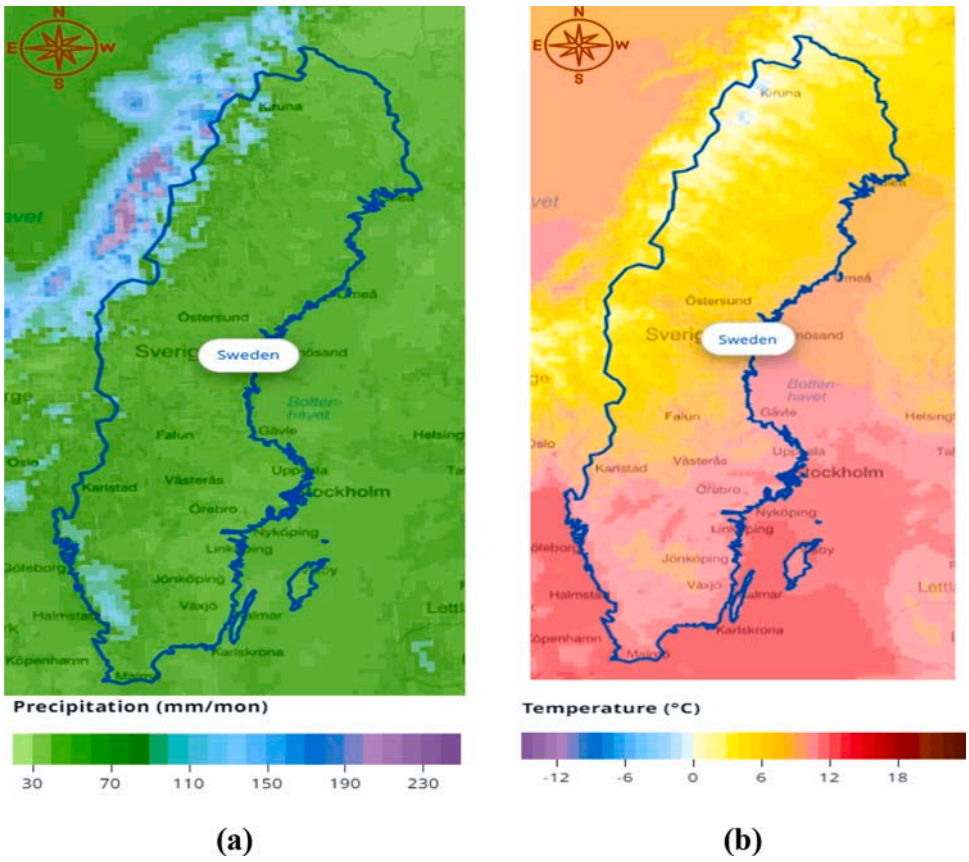

Fig. 1. Absolute values of (a) Precipitation and (b) Temperature for the period 2071–2100 based on emissions scenario RCP8.5, adapted from (SMHI).

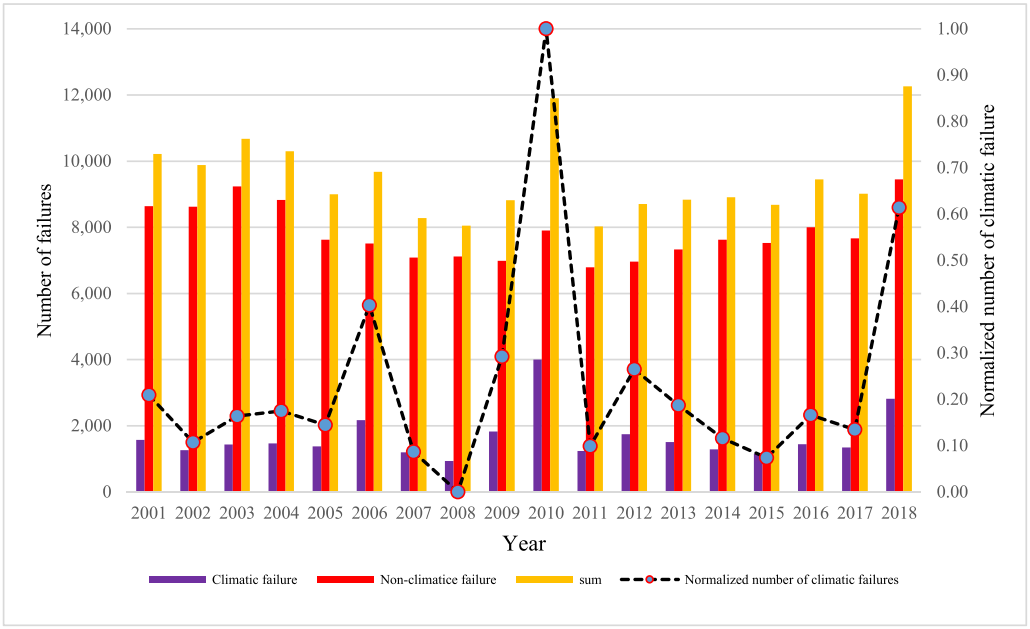

Fig. 2. The annual failure count of assets in two distinct categories (Climate failure and non-climate failure) over the whole of Sweden.

non-climatic. The normalized number of climate failures (The dashed black line) illustrates fluctuations over the period of 18 years over the whole of Sweden, with a notable increase in the total number of failures observed in the year 2010. Specifically, 2010 recorded the highest number of failures, with 4001 climatic failure occurrences for the entire network.

The Scaling of variable, number of failures in different years, are calculates based on the following equation:

$$x' = \frac{x - \min(x)}{\max(x) - \min(x)} \quad (1)$$

Where: x' is the normalized value, x is the value of the variable,

$\min(x)$ and $\max(x)$ are the minimum and maximum values of the variable respectively. In the case of this manuscript the variable for this Figure is the number of failures in different years.

Moreover, various meteorological indicators have been considered to understand the underlying failure causes for the year 2010. For instance, the following metrics have been considered as given in Table 1:

Maximum 24 h precipitation – average of the year's or season's greatest 24 h precipitation for 60 stations across Sweden

Days with at least 40 mm – average of the number of observations per year with a daily perception of at least 40 mm for 60 stations across Sweden.

The absolute maximum 24 h precipitation – the year's greatest 24 h precipitation in Sweden (based on all stations) (SMHI, 2015)

These metrics for 2010 received higher value compared to other years. In addition, our analyses showed that the whole of Sweden experienced extreme cold weather conditions in the same year.

Furthermore, Fig. 3 provides insight into the distribution of failures throughout the months which indicates that a significant portion of the total failures occurs during the cold months in Sweden.

2.2. Future climate scenarios

Representative concentration pathways (RCPs) are utilized to gain insights into the potential range of climate outcomes and can devise strategies to mitigate the impacts of climate change (Bienvenido-Huertas David et al., 2021). Various scenarios, including RCP2.6, RCP4.5, RCP6.0, and RCP8.5, describe projected radiative forcing levels by the year 2100 in watts per square meter.

In RCP2.6, greenhouse gas emissions start to decline in the year 2020 to reach zero at the end of the century; in RCP4.5, emissions continue to increase around 2040 and decline afterward; while in RCP8.5 emissions continue to increase until the end of the century. The estimated global warming to the end of the century compared to today is roughly 1 °C, 2 °C, and 4 °C for RCP2.6, RCP4.5 and RCP8.5, respectively (IPCC, 2014).

2.3. Projected change in meteorological parameters in Sweden

The information about projected climate change is based on results from a number of regional climate model (RCM) simulations from EURO-CORDEX, performed on 12.5*12.5 km horizontal grid spacing and subsequently bias-adjusted. The RCMs are forced with data from various global climate models (GCMs) at the resolutions of 50–200 km.

SMHI (Swedish Meteorological and Hydrological Institute) projects climate change impacts under different RCPs and the following conclusions have been made for Sweden:

1. The number of days with hot temperatures (above +25-degree) will increase, especially in the south,
2. The number of days with zero-crossings will decrease in the south and increase in the north during winter,
3. Precipitation is generally projected to increase but with variations across seasons and regions,
4. Fewer cold days mean that a larger proportion of the precipitation will fall as rain instead of snow; snowfall intensity, however, may increase.

Based on our research analysis performed in CliMaint research project (Garmabaki, 2019), Fig. 4 shows the projected changes in winter temperature for four cities in Sweden (Kiruna: northwest; Luleå: northeast; Stockholm: middle; Göteborg: southwest) according to three different RCP scenarios. It is evident that the warming is larger in northern Sweden (up to 10 °C) than in southern Sweden (up to 5 °C) according to RCP8.5. In Stockholm, the average winter temperature is projected to increase from below zero to above zero at the end of the century, except in RCP2.6 to the end of the century. Fig. 5 shows the projected changes in winter precipitation. Precipitation is projected to increase everywhere, somewhat more in the west than in the rest of the country.

Table 1
Climate indicators for different years for whole of Sweden (SMHI).

Year	Yearly precipitation (mm)	Average temperature (°C)	Extreme precipitation	
			Max daily	Days with at least 40 mm
2001	714	4.49	37.5	0.43
2002	640	5.19	33.3	0.25
2003	614	4.98	33.7	0.25
2004	678	4.86	34.6	0.23
2005	640	5.22	30.4	0.08
2006	734	5.62	36.0	0.34
2007	701	5.4	33.3	0.28
2008	733	5.61	34.6	0.35
2009	686	4.79	37.3	0.29
2010	**687**	**2.93**	**40.2**	**0.51**
2011	735	5.69	36.1	0.33
2012	798	4.43	33.5	0.22
2013	587	5.04	29.5	0.11
2014	695	6.21	35.0	0.38
2015	724	5.91	30.5	0.13
2016	594	5.39	31.5	0.21
2017	710	5.15	30.6	0.13
2018	532	5.63	28.5	0.13
Max value	798	6.21	40.2	0.51
Min value	532	2.93	28.5	0.08

2.4. Climate change adaptation strategies

Climate adaptation aims to reduce climate risks and vulnerabilities of existing systems. Adaptation strategies for railway asset infrastructures can be grouped in (i) protect, (ii) accommodate, (iii) retreat, and (iv) avoid, which are described as follows (IPCC., 2022). Fig. 6 presents climate adaptation strategies for railway infrastructure endangered by sea level rise.

Protect is a reactive strategy employed to safeguard people, property, and railway infrastructure from the impacts of natural phenomena. Protecting railway infrastructure often involves implementing structural mechanisms such as barriers, embankments, and protective walls. However, as environmental risks evolve and vulnerabilities increase, solely relying on this approach may become financially impractical and yield limited long-term effectiveness, especially in highly susceptible locations (IPCC., 2022; Tyler, 2015).

Accommodate represents an adaptive strategy that enhances the resilience of the railway infrastructure during varying environmental conditions. This approach entails making suitable adjustments to the railway infrastructure to effectively address challenges. Accommodation may include retrofitting railway infrastructures to enhance resilience against potential consequences of changing climate conditions. In essence, the accommodate strategy strives to ensure railway infrastructure's sustained functionality and durability while addressing a broader range of natural hazards and uncertainties (IPCC., 2022; Tyler, 2015).

Retreat involves making deliberate decisions to withdraw, relocate, or abandon private or public assets that face vulnerabilities. The retreat strategy aims to minimize dependence on structural protection for railway infrastructure, discourage development in areas prone to environmental changes, and strategically plan for relocating buildings and railway facilities to regions with lower or no risk (IPCC., 2022; Tyler, 2015).

Avoid strategy focuses on preventing new developments in areas prone to hazards and risks. This includes locations where there is a current low risk but an expected increase in risk over time. Future "no

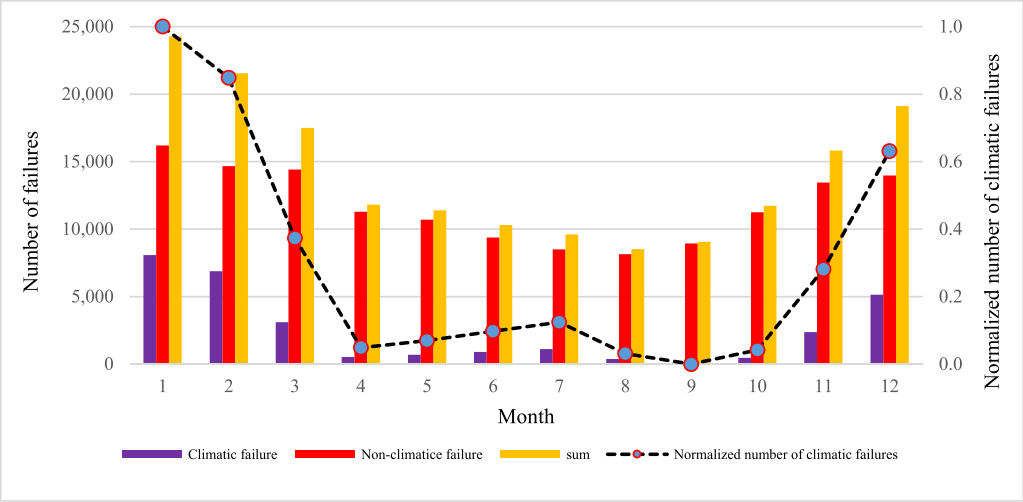

Fig. 3. The monthly failure count of S&Cs in two distinct categories.

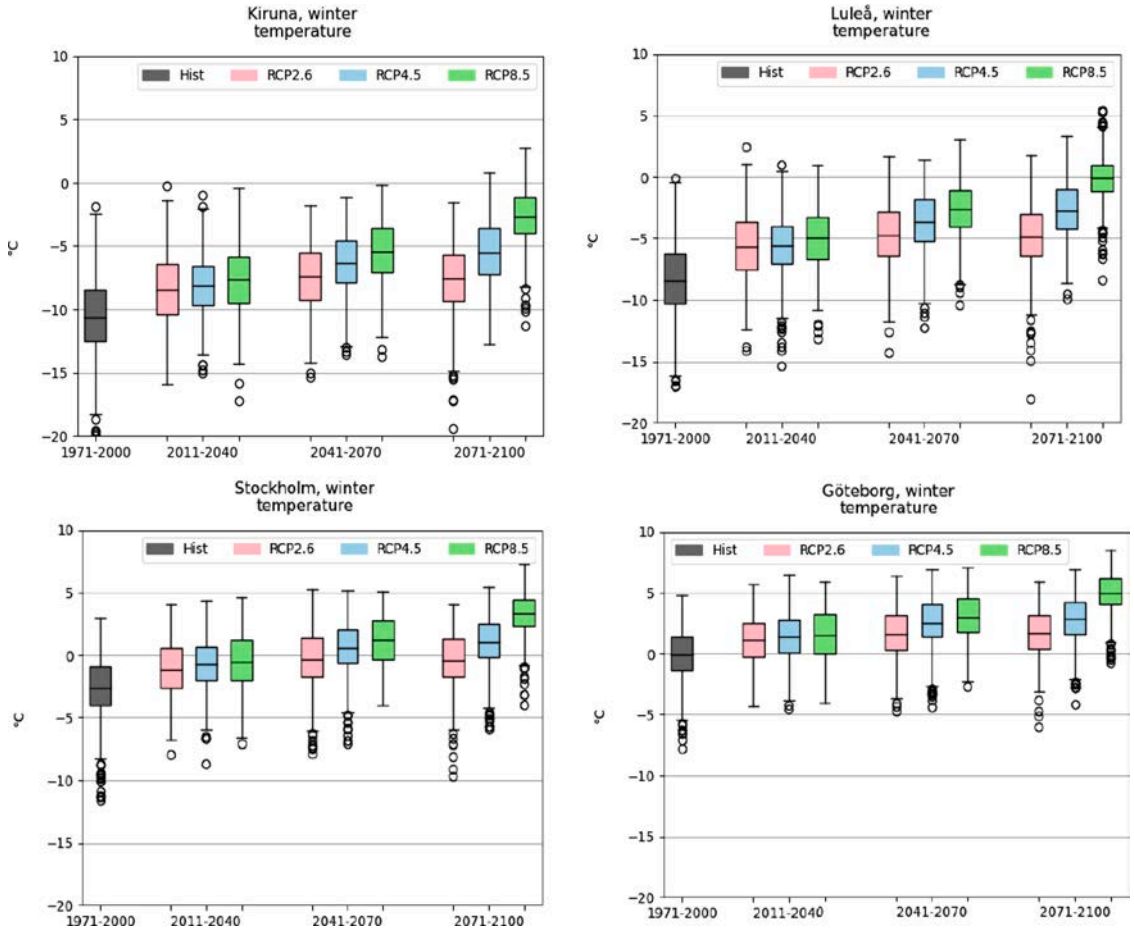

Fig. 4. Projected winter temperature (°C) in four Swedish cities in the historical period 1971–2000 grey boxes, and the periods 2011–2040, 2041–2070, and 2071–2100 according to RCPs RCP2.6 (pink boxes), RCP4.5 (blue boxes) and RCP8.5 (green boxes). The boxes represent the interquartile range (IQR) of the data, the line within represents the median, the whiskers extend from the box by 1.5xIQR. Data points outside the whiskers are marked by circles.

build" areas are identified and incorporated into local government planning documents. Diverse planning tools are utilized to make informed decisions that discourage development in moderate to high risk regions. As part of the avoidance strategy, options such as land acquisition or the transfer of development potential to safer areas are considered. (IPCC., 2022; Tyler, 2015)

3. Proposed methodology

Climate impact assessment is a preliminary step to identify/select and implement the right climate adaptation strategies. The main objective of this paper is to assess how climate change impacts asset reliability and make an effective methodology to explore how

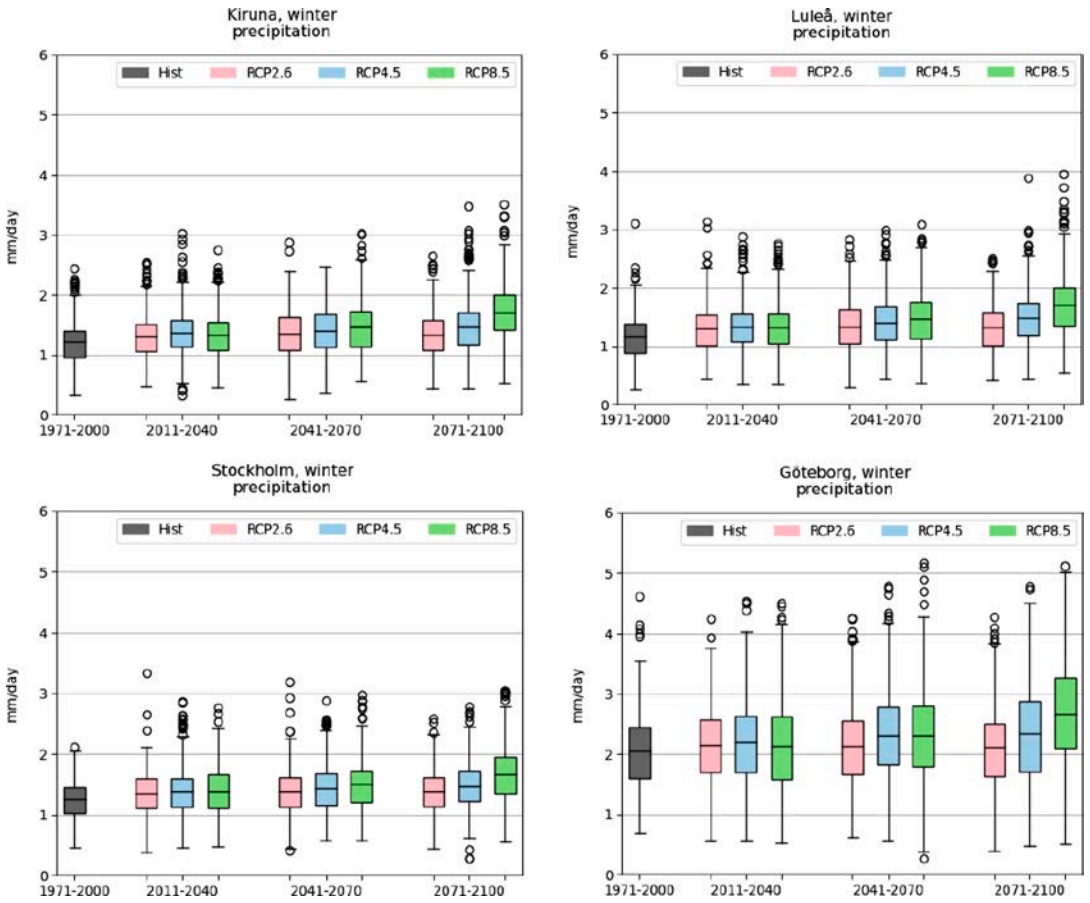

Fig. 5. Projected winter precipitation (mm/day) in four Swedish cities in the historical period 1971–2000 grey boxes, and the periods 2011–2040, 2041–2070, and 2071–2100 according to RCPs RCP2.6 (pink boxes), RCP4.5 (blue boxes) and RCP8.5 (green boxes).

Fig. 6. Different climate change adaptation strategies for endangered railway infrastructures by sea level rise adapted from (German Development Cooperation, 2009).

infrastructure asset managers can adapt their maintenance strategies accordingly. The reliability assessment methodology is followed to achieve this aim, as depicted in Fig. 7.

Cox PHM is a technique for integrating meteorological parameters and conducting reliability assessments. This model allows for the consideration of various covariates and failure history, enabling predictions of how different climate scenarios will affect the hazard rate and, consequently, asset reliability. This information empowers infrastructure asset managers to plan maintenance activities more efficiently, minimize downtime, and optimize asset utilization (Si et al., 2011). The subsequent subsections will discuss different phases of the methodology.

3.1. Phase 0: Data gathering

Data collection and information were challenging tasks. For instance, Trafikverket (Swedish Transport Administration) failure reporting system is not designed to collect information related to climate-based failure; thus, tracking the underlying failure cause was tedious. Required data have been collected from various databases, including S&Cs' failure databases, asset registry data, meteorological databases, etc.

3.1.1. Selecting the infrastructure asset of study

Switch and Crossing (S&C) is one critical asset in the railway infrastructure networks as shown in Fig. 8. When the switching mechanism is initiated, the switchblade moves to its opposite position in order to divert the train in another direction. Many failures can cause S&C malfunction, and black box approaches have been followed while performing failure analyses.

3.1.2. Failure data collection and pre-processing

The main databases from Trafikverket, which are essential for model development, are described as follows. All these data sources contain information directly related to asset failures, inspection, aging and degradation, etc. Therefore, one of the critical tasks is to aggregate these disparate data sources for the selected assets to perform a comprehensive analysis.

Asset Register (BIS): contains the technical description and the

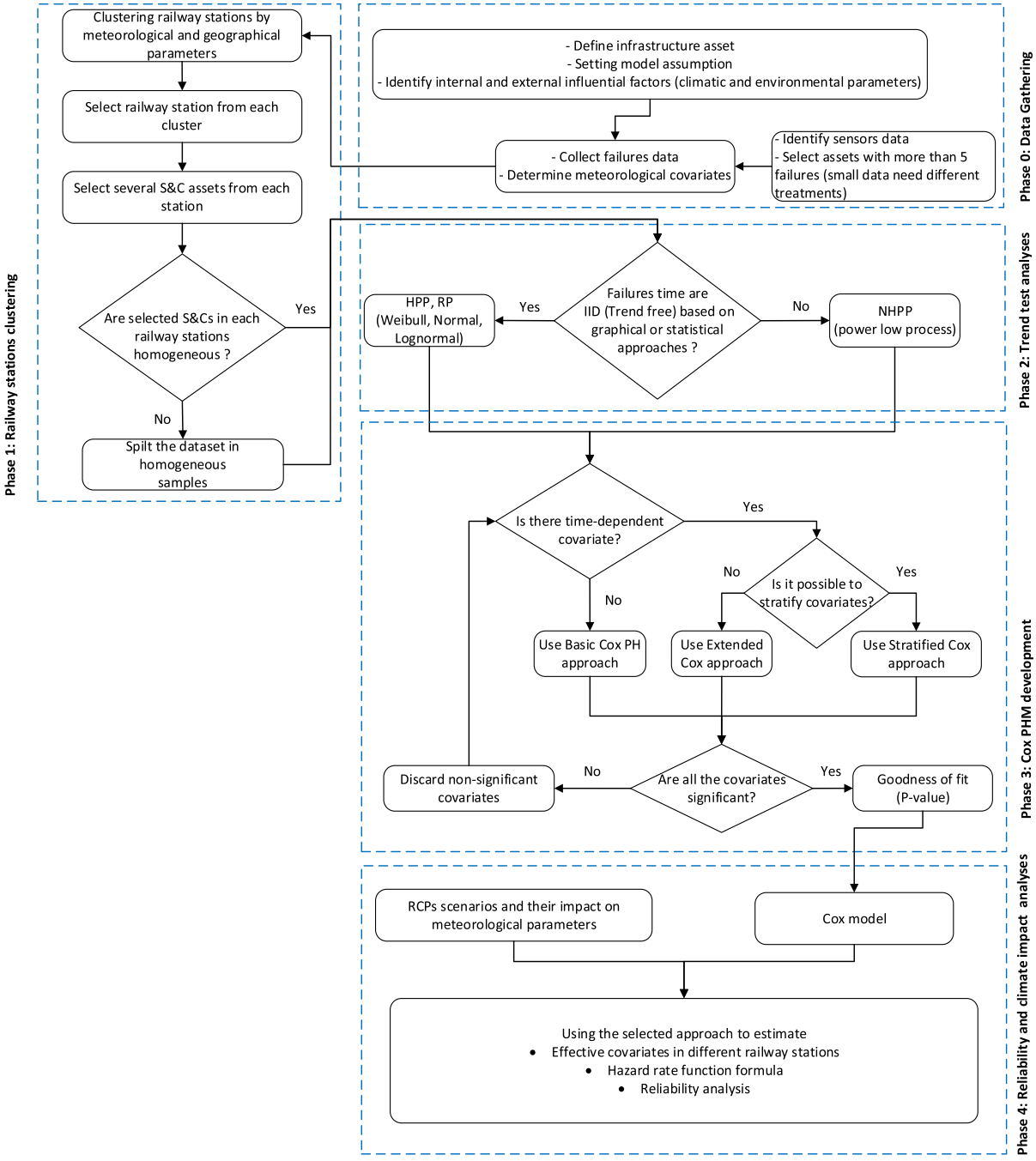

Fig. 7. Proposed research methodology for reliability analysis associated with climate variables.

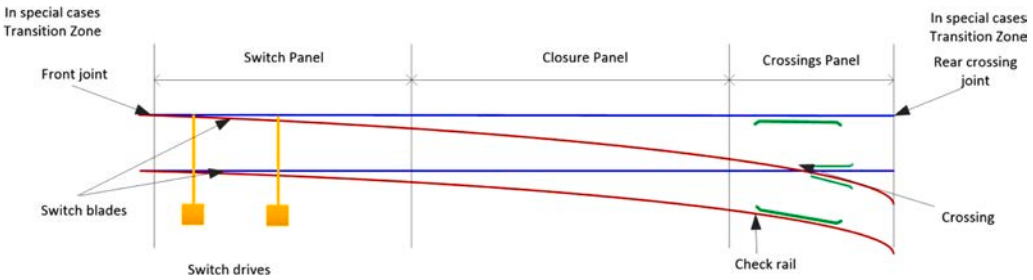

Fig. 8. Illustration of Switches and Crossings (Nissen, 2009).

localization of all the Track assets and components. This database is regularly updated based on the changes made to the assets.

Work Orders (OFELIA): supports track maintenance processes and contains:

- Track failures and incidents,
- Maintenance reports provided by the subcontractors, including, e.g., the cause of each intervention, their date, and the actions they performed in track. This database also consists of a cause code; however, this database is not designed to collect climate/environmental parameters at the time of failure. In several incidents, maintenance experts described the situation in text.

One of the important steps in this analysis is to distinguish between asset failure and whether it is caused by climatic impact or not. To tackle the issue, the records representing climatic failure have been recognized through failure cause code or performing text mining. For text mining, a wide range of keywords have been identified by consulting with railway experts.

Furthermore, there is a need to integrate different Trafikverket databases mentioned above and associated meteorological information. To do so, a new feature has been developed and represented by "Climate_id". In other words, Climate_id is performing failure classification task and integration task. It may be noted that for failure classification, we did not distinguish between physical/structural failures or failures due to loss of functionalities.

In addition, the main climatic factors affecting the railway infrastructure have also been identified and shown in Table 2. The snow and ice category has the largest portion of failures with a climatic cause, and about 16.5 percent of these failures have led to interruption in traffic flow, which can associated with significant costs.

3.1.3. Meteorological data collection and analysis

To gain insights into the potential impacts of climate change on the railway system, it is crucial to understand how the climate is evolving. Specifically, it is vital to identify climate indicators that are likely to affect the railway infrastructure functionalities. One reliable source of meteorological parameters, such as temperature, relative humidity, precipitation, wind speed, and snow depth, is the SMHI website, which provides open-source data. These parameters can serve as valuable inputs for analyzing the potential climate-related impacts on the railway system. To prepare the dataset for analysis (as depicted in Fig. 9), various weather stations may be situated in the vicinity of the selected railway station. To determine the most relevant weather station for the specific railway section of interest (S&Cs), measurements of the distances between the weather stations and the railway station are taken into account. By selecting the closest weather station, data that is most representative of the local climate conditions affecting the railway can be obtained. The analysis process involves synchronizing two distinct databases: one containing the operational features of the S&Cs sourced from Trafikverket and the other comprising the meteorological data obtained from SMHI. To effectively combine these databases, the failure times recorded in the first database are utilized as reference points. A cohesive and unified dataset is created by aligning the failure times, enabling comprehensive examination of the relationship between railway failures and meteorological conditions.

Table 2
Frequency of failures and traffic interruption percentage.

Root cause	Climate_id	# events	# events resulted in traffic interruption
Climatic	Abnormal temperature	4 363	461
	Buckling	15	11
	Fire	228	23
	Heavy wind / Storm	88	11
	Natural events	260	212
	Slippery track	10	0
	Snow and ice	23 501	3 876
	Storm / Snowstorm	1276	148
Non-climatic	Other failures	140 892	15 453
	Total	**170 633**	**20 194**

3.2. Phase 1: Clustering approach using K-Means

The K-Means algorithm is an unsupervised machine learning method which is utilized to divide the whole of railway stations considered into different clusters. This approach consists of the following steps (see Fig. 10):

Step 1: Select the number of clusters (K)
Step 2: Initialize the centroids of each cluster randomly
Step 3: Assign each data point (each of railway station) to the nearest centroid based on the Euclidean distance between the data point and the centroid
Step 4: Recalculate the centroid of each cluster as the mean of all the data points assigned to that cluster.
Step 5: Repeat steps 3 and 4 until the centroids no longer change or until a maximum number of iterations is reached.

The algorithm outputs are the final clusters containing the members assigned to the same centroid.

3.3. Phase 2: Trend assessment and underlying process

The trend assessment is a method used to evaluate whether there is a trend or pattern in the failure times of a system or component. Garmabaki et al. (2016); Louit et al. (2009) have described several statistical tests that can be used to evaluate trends in cumulative failure time, including the Laplace trend test, Military Handbook test, and Anderson–Darling test. These tests evaluate the data for a monotonic trend, meaning a consistent increase or decrease in the cumulative failure time over time. In statistical trend tests, the null hypothesis is a statement of no trend (H0) versus monotonic trend (H1). If the time between failures satisfies the assumption of being independent and identically distributed (IID), the homogeneous Poisson process (HPP) or renewal process can be implemented. To verify this assumption, the serial correlation test, a graphical method, can be employed. For more details of standard reliability analyses of repairable systems, see (Garmabaki et al., 2016). On the other hand, if the null hypothesis (a statement of no trend (H0)) is rejected, a non-homogeneous Poisson process (NHPP) will be utilized to show the behavior of the system.

3.4. Phase 3: Cox proportional hazard model development

Three different types of Cox PHM have been proposed in the methodology framework (see Fig. 7). The mathematical structure of each model is described as follows:

3.4.1. Conventional Cox model

The Cox PHM is written in terms of the hazard model formula shown in Eq. (2). This model expresses the hazard at time t for an asset with a given specification of a set of explanatory variables denoted by. The X represents a vector of predictor variables to predict an asset's hazard. The Cox model formula says that the hazard at time t is the multiplication of two quantities. The first of these $h_0(t)$, is called the baseline hazard function. The second quantity is the exponential expression e to the linear sum of $\beta_i X_i$, where the sum is over the p explanatory X variables (Bendell A et al., 1991; Cox, 1972; Kleinbaum & Klein, 1996).

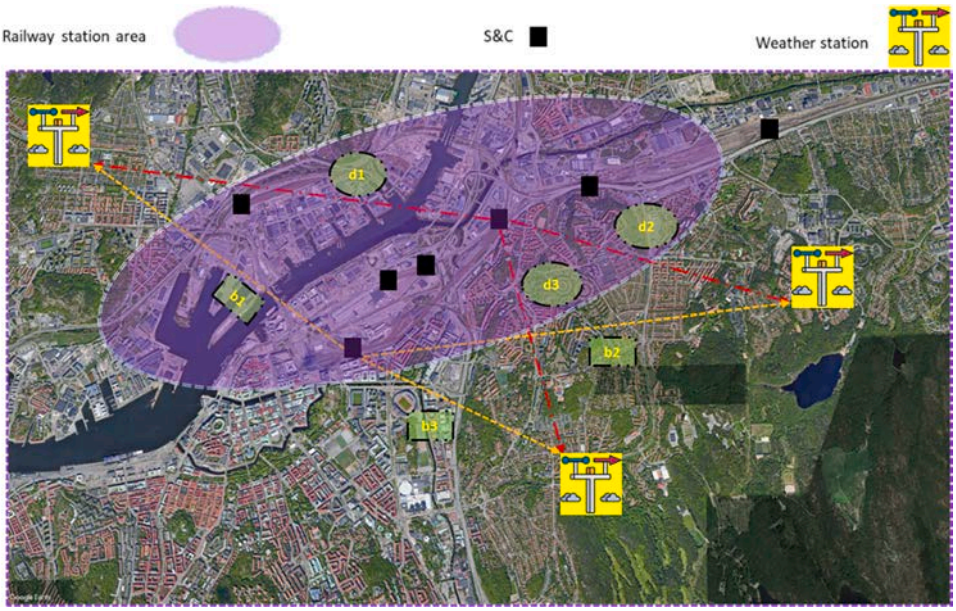

Fig. 9. Position of assets in railway stations and distance between assets and weather stations (Google earth).

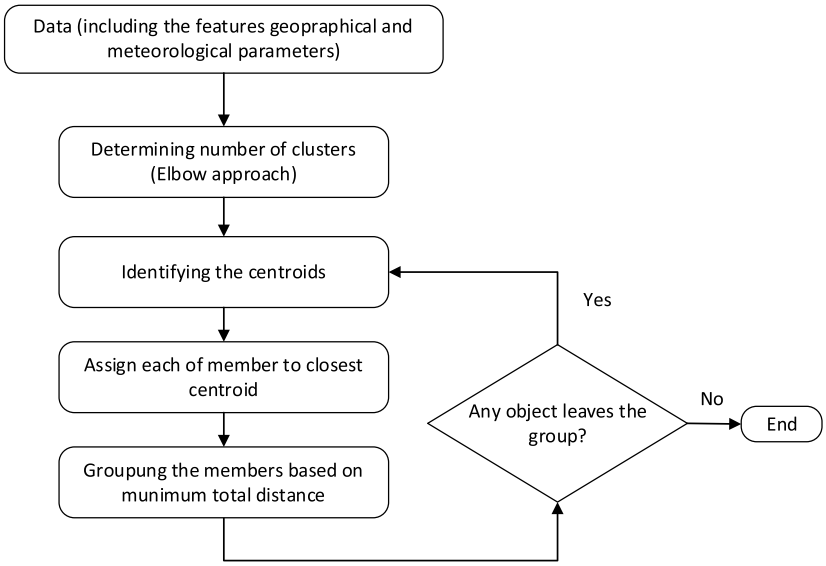

Fig. 10. Flowchart for implementing the process of K-means clustering.

$$h(t,\ X) = h_0(t)e^{\sum_{i=1}^{p}\beta_i X_i} \tag{2}$$

A hazard ratio (HR) (See Eq. (3)) is the hazard for one asset (unit) divided by the hazard for a different asset. The two assets being compared can be distinguished by their values for the set of predictors, X's. The HR can be written as the estimate of $h(t,\ X_1)$ divided by the estimate of $h(t,\ X_2)$ where $h(t,\ X_1)$ denotes the set of predictors for one asset, and $h(t,\ X_2)$ for the other one.

$$HR = \frac{h(t,\ X_1)}{h(t,\ X_2)} = \frac{h_0(t)e^{\sum_{i=1}^{p}\beta_i X_{2i}}}{h_0(t)e^{\sum_{i=1}^{p}\beta_i X_{1i}}} = e^{\sum_{i=1}^{p}\beta_i (X_{2i}\ -X_{1i})} = \theta \tag{3}$$

Where $X_1 = (X_{11},\ X_{12},\ X_{13},\ \ldots,\ X_{1p})$, $X_2 = (X_{21},\ X_{22},\ X_{23},\ \ldots,\ X_{2p})$, and θ is a constant.

The HR is independent of t, and is a constant value. To use PHM, PH assumption should be verified that the hazard ratio is constant. In case of violating PH assumption, there are two alternatives, including a stratified Cox model (SCM) or an extended Cox model (ECM).

3.4.2. Stratified Cox Model

When the PH assumption is not satisfied for a particular covariate, a simple solution is to use the stratified Cox model (SCM). In this model, data are stratified into subgroups or strata, and the Cox model is applied to each subgroup or stratum (Sarkar et al., 2017). The model is presented by Eq. (4):

$$h_g(t,\ X) = h_{0g}(t)e^{\sum_{i=1}^{p}\beta_i X_i},\ g = 1,\ 2,\ 3,\ \ldots,\ k \tag{4}$$

$Z_1,\ Z_2,\ Z_3,\ \ldots,\ Z_k$, do not satisfy PH assumption and $X_1,\ X_2,\ X_3,\ \ldots,\ X_p$, satisfy PH assumption, k is the total number of combinations (or strata) formed after categorizing each of the Z_i.

In SCM, covariates which do not satisfy the PH assumption are not considered explicitly. In addition, the baseline hazard function $h_{0g}(t)$ is

allowed to be different for each stratum. However, the coefficients β_1, β_2, β_3, …, β_p are the same for each stratum; this property of the model is called no-interaction assumption. Another type of SCM allows interaction between the variables that do not satisfy the PH assumption and the other covariates. This mathematical modeling of such a SCM is presented by Eq. (5):

$$h_g(t,\ X) = h_{0g}(t)e^{\sum_{i=1}^{p}\beta_{ig}X_i},\ g = 1,\ 2,\ 3,\ \ldots,\ k \tag{5}$$

3.4.3. Extended Cox model

Incorporating time-dependent variables violates the PH assumption, so an extended Cox model (ECM) can be utilized. In contrast with conventional Cox PHM, the exponential part of ECM includes both time-independent variables X_i, and time-dependent variables $X_j(t)$, where δ_j is a coefficient for time-dependent covariates, as given in Eq. (6).

$$h(t,\ X(t)) = h_0(t)e^{\left[\sum_{i=1}^{p_1}\beta_i X_i + \sum_{j=1}^{p_2}\delta_j X_j(t)\right]} \tag{6}$$

3.5. Phase 4: Reliability assessment

The reliability function, also known as the survival function, is the probability that an item will survive beyond a given time, and it is the complement of the cumulative distribution function (CDF) or the probability of failure. The relationship between the hazard rate which has been described in the previous section, and the reliability function is as Eq. (7).

$$R(t,\ X\ ) = \exp\left(-\int_0^t h(x,\ X)dx\right) \tag{7}$$

Mean time between failures (MTBF) as one of the important indicators for assessing the effect of various scenarios can be used. Eq. (8) shows the relationship between the reliability and MTBF.

$$MTBF(t,\ X\ ) = \int_0^\infty R(u,\ X\ )dt \tag{8}$$

4. Results and discussion

To validate the proposed framework and assess the climate change impacts and its variability on Sweden railway infrastructure assets, S&Cs have been selected for the analyses. For this aim, 40 railway stations are chosen to explore and cover a wider range of climate variability based on geographical location, data availability, including metrological and asset O&M data.

4.1. Clustering urban railway stations

The temperature statistical features, including mean, standard deviation (std), skewness, kurtosis, as well as the geographic coordinates (i.e., latitude, longitude) and their height above sea level, have been collected for selected 40 urban railway stations. K-means has been utilized as an unsupervised machine learning approach to cluster the urban railway stations based on the selected features. For implementing the clustering steps, the Elbow approach is applied to identify the optimal number centroid, which is an initial input of K-Means clustering approach. As shown in Fig. 11, the optimal number of clusters for the given dataset was determined to be four.

Using this parameter (K=4), the K-Means technique was implemented by Python 3.8. Fig. 12 shows the outcome of the K-mean clustering process. With clustering, 40 urban railway stations are distributed over the identified four clusters. The clusters shown in the figure are divided by border, and each cluster is indicated by four different colors,

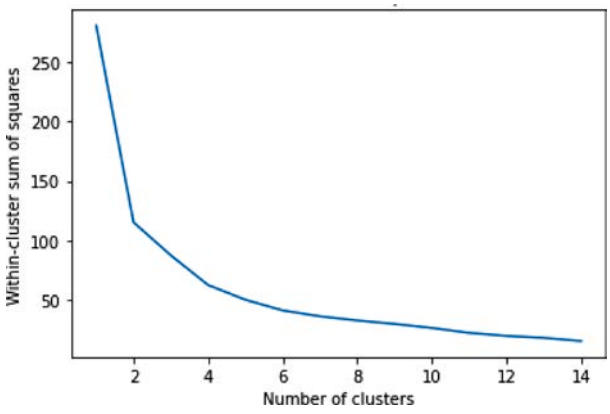

Fig. 11. Using the Elbow method to determine the optimal number of clusters for K-Means algorithm.

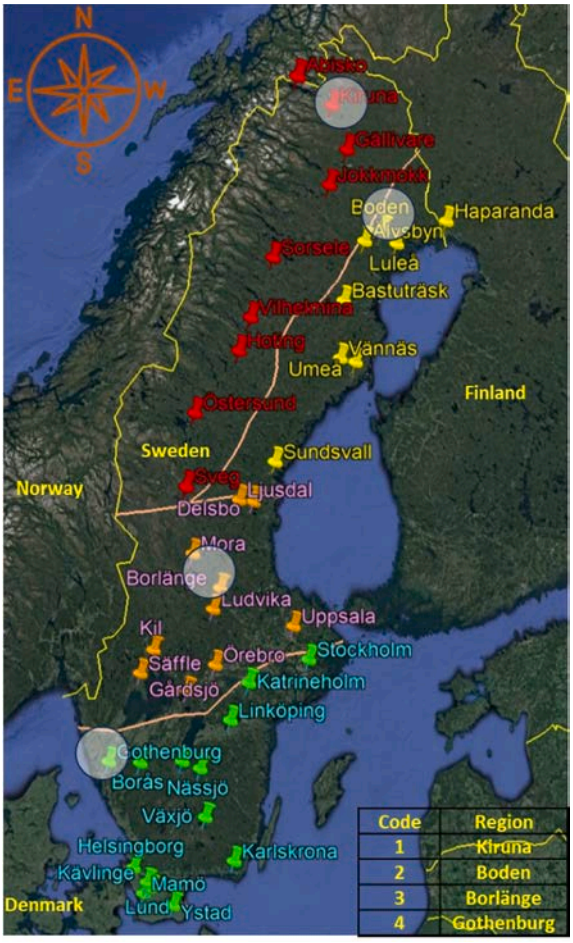

Fig. 12. Different climate zones and related railway stations over the Swedish's railway network and 4 selected railway stations (Google earth).

including red (cluster 1), yellow (cluster 2), purple (cluster 3), and light blue (cluster 4).

For reliability analyses, four stations, encompassing Kiruna, Boden, Borlänge, and Gothenburg, have been selected based on railway infrastructure expert opinions as given in Fig. 12.

Thereafter, failure, inspection, and asset registry data for the assets located in the above four stations have been collected, and climatic features, including Climate_id, have been extracted. We have selected a sample of 25 S&C from the population of assets located in four stations

Table 3
Assets' region, their location, type of selected S&Cs and number of associated failures.

Station region	Cluster No.	Selected type of S&C	Final No. failures for analysis	Number of selected S&C
Kiruna	1	DKV	314	3
Boden	2	EV	297	8
Borlänge	3	DKV	305	5
Gothenburg	4	DKV	968	9

based on the number of failure records, type of S&C, etc. see Table 3.

The failure data of S&Cs includes features such as S&Cs type and its characteristics, failure time, response time, maintenance duration, and maintenance area. These data were collected from various datasets, as discussed in Section 3.1, and were integrated for the selected infrastructures over 18 years, from 2001 to 2018. Accordingly, Bartlett's test is employed as a statistical tool to examine the null hypothesis, H0, which assesses that the variances of all k populations are equivalent while considering the alternative hypothesis, H1, that at least two of these variances are distinct (Garmabaki et al., 2016). For the case of this study, since failure/repair data originate from multiple S&Cs for each region, Bartlett's test are used, and the results for each region are presented in Table 4. The results show that there is not enough evidence to reject the null hypothesis.

4.2. Determining baseline hazard

According to the proposed methodology, in phase 2, the baseline for the Cox model can be determined by implementing the trend test (graphical and/or statistical trend test). As depicted in Fig. 13, the selected assets for two failure modes which are divided into two categories by climate_id variable, exhibit a trend. It should be mentioned that statistical tests such as Military handbook, Laplace, and Anderson-Darling also have confirmed graphical test results. Therefore, power law process (PLP), a specific form of the NHPP, is employed to estimate the baseline hazard.

The parameters of the PLP, including shape (β) and scale (θ), are estimated using Minitab software 20 in accordance with the NHPP and these parameters for different regions in three statuses including the two failure modes and integrated data are presented in Table 5.

4.3. Hazard rate associated with covariates impact

Meteorological variables (covariates), including Air temperature (X_1), Relative humidity (X_2), Precipitation (X_3), and Wind speed (X_4) were collected from the SMHI databases for the same duration of failure data. We have considered several other meteorological features like snowfall; however, they were excluded from the analysis due to the quality and quantity of data. A detailed description of the selected meteorological parameters can be found in Table 6.

Table 7 displays a sample of datasets designed to develop the Cox PHM for one of the selected S&C from the Kiruna region and its associated covariates. Two distinct categories of failures were identified based on the data-gathering and pre-processing steps as Climate_id parameter (see Section 3.1). This table further encompasses the considered covariates (X1-X4) and the duration between successive failures (TBF). The average value of meteorological parameters has been calculated by collecting the last 24-hourly data prior to the failure time.

Table 4
Assessment of Bartlett's test for different regions.

Station region	Cluster No.	P-value	Null hypothesis, at 5 % significant level
Kiruna	1	0.060	Not rejected
Boden	2	0.254	Not rejected
Borlänge	3	0.237	Not rejected
Gothenburg	4	0.663	Not rejected

Table 8 presents the results obtained from the regression Cox model, which was implemented by STATA15, displaying the coefficients (β_i) and their corresponding effects. The null hypothesis Cox PHM assumes that the covariates have no impact and the P-value significance level is set to 0.15. For Kiruna region, covariates X_2 and X_3 rejected the null hypothesis, indicating these covariates have a significant impact. Subsequently, in a second step, the effects of these two covariates on the model were re-evaluated, confirming their selection as influential factors in the Cox model. This procedure was repeated for the remaining regions, and driving covariates have been identified. Notably, the relative humidity and precipitation were determined as the effective covariates for the Kiruna region, while wind speed emerged as the influential covariate for Borlänge. The effective covariates selected for the Gothenburg region included temperature and relative humidity. Conversely, the assessment has revealed that the selected covariates had no significant effect on the Boden region.

After identifying appropriate Cox PH model parameters, the Schoenfeld test has been used to evaluate the goodness-of-fit and examine the model's residuals (Abeysekera & Sooriyarachchi, 2009; Moreau et al., 1986; Schoenfeld, 1980). The null hypothesis of the Schoenfeld test declares that there is no time dependence for the parameter being examined. As shown in Table 9, the results for the significant level of 0.05 demonstrate that all covariates meet the PH assumption.

According to the proposed methodology, the hazard rate formula has been developed, including baseline and exponential terms. Table 10 presents hazard rate formulas for the non-climatic ($h_0(t,\ X)$) and climatic ($h_1(t,\ \mathbf{X})$) failure modes.

4.4. Interpretation of effective covariates

Based on the analysis conducted in the previous section, the effective meteorological covariates for the selected S&Cs have been determined. For instance, in the Kiruna region, the coefficient for precipitation is found to be about 1.12. This implies that one-unit increase in precipitation can result in a more than three-fold increase in the hazard ratio ($HR = \exp(1.12) = 3.06$). In Borlänge, wind speed has been identified as a significant parameter influencing the hazard rate. Therefore one-unit increase in wind speed leads to a more than 16 percent increase in the hazard ratio ($HR = \exp(0.149) = 1.16$). These findings highlight two important observations. Firstly, the dominant meteorological parameters affecting the infrastructure can vary from place to place depending on the region's meteorological and geographical features. Secondly, the magnitude of the effect for different covariates can differ significantly. These results underscore the need for region-specific consideration of meteorological factors in infrastructure management.

Analyses have revealed that for the selected assets in Boden and Gothenburg, selected covariates did not significantly impact the hazard rate. A definitive conclusion that these meteorological parameters do not affect S&Cs is challenging. By incorporating additional covariates that capture the operational context and other relevant variables, such as traffic volume, the number of trains passing through the area, a more comprehensive understanding of the relationship between meteorological parameters and infrastructure assets and physical properties can lead to more accurate climatic impact outcomes. Data quality and the number of records are two other impact factors while performing analysis. Hence, the failure reporting system may need to be enriched to capture more information regarding environmental impacts considering future climate change failure causes. Moreover, assessing climate impacts is challenging for the assets located in rural areas due to the longer distance between the asset and the weather station, leading to a wider confidence interval for the reliability assessment. Utilizing new data-gathering technologies, such as IoT devices, is an approach to improve data quality and accurate analysis.

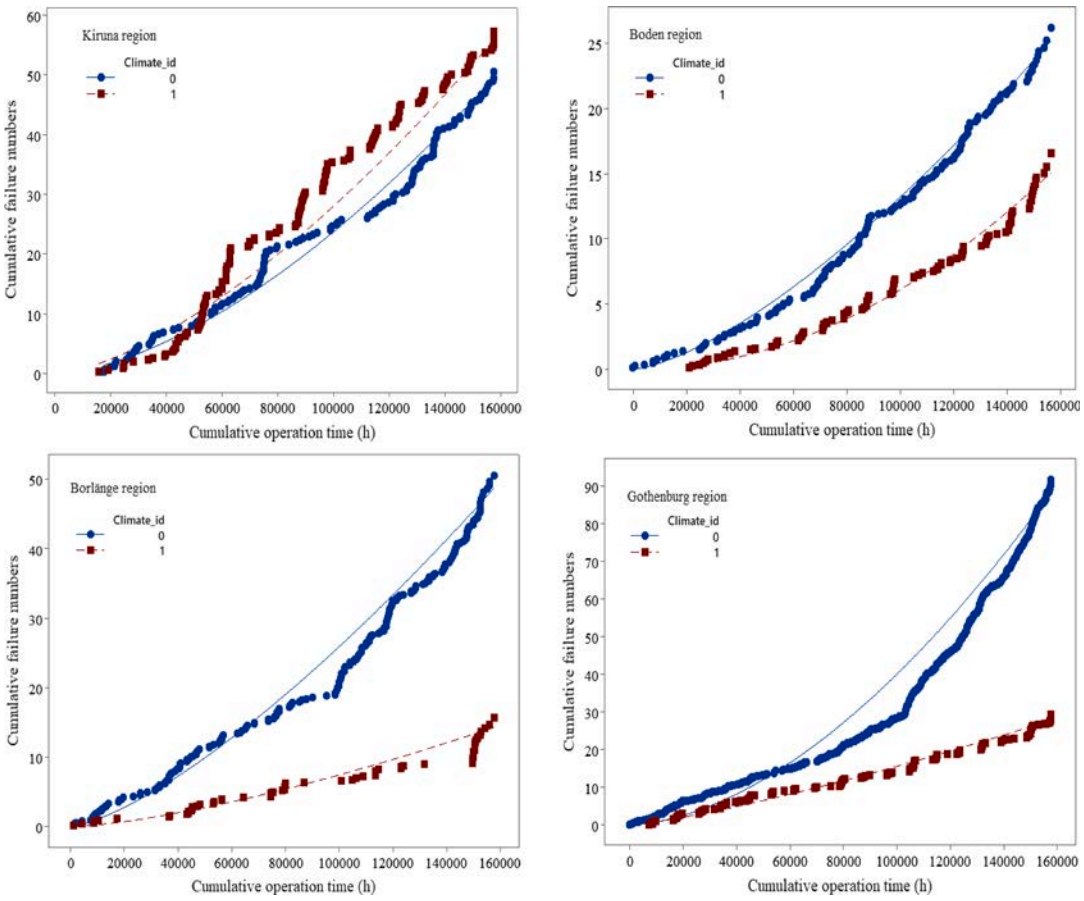

Fig. 13. Failure behavior of the assets with considering two failure modes.

Table 5
Power law process parameters including shape and scale for various regions.

Region	Climate_id	Shape parameter (β)	Scale parameter (θ)
Kiruna	0*	1.62	14,120
	1*	1.52	11,136
	Integrated data	1.56	8011
Boden	0	1.44	16,705
	1	2.02	40,784
	Integrated data	1.61	15,820
Borlänge	0	1.39	9558
	1	1.43	24,529
	Integrated data	1.40	8105
Gothenburg	0	1.74	12,020
	1	1.27	11,618
	Integrated data	1.60	8078

* 0: non-climatic, 1: climatic

Table 6
Description of selected meteorological covariates.

Parameter	Unit	Frequency	Range
Air temperature (X_1)	°C	hourly	−60 to +40
Relative humidity (X_2)	%	hourly	0 to 100
Precipitation (X_3)	mm	hourly	≥ 0
Wind speed (X_4)	m/s	hourly	≥ 0

4.5. Sensitivity analysis

Based on the World bank group and SMHI data, the precipitation projects to change according to different RCPs, the following analyses are implemented to assess the sensitivity of selected urban railway S&Cs (SMHI; World bank group, 2021). Fig. 14 illustrates the influence of varying precipitation values on the reliability of assets within the Kiruna region. This graph provides a clear description of the impacts of increasing precipitation value on the reliability of assets. As precipitation values increase, the reliability of assets decreases, resulting in a higher number of failures and increased O&M costs.

Fig. 15-a specifically focuses on the effect of the precipitation covariate on the median time of reliability. As depicted in this figure, the reliability analysis reveals that the median reliability for the scenario (X3= 0.00 mm) is estimated to be 8754 hours. This finding indicates that, for selected assets, the probability of experiencing failure or required repair before reaching 8754 hours of operation, is 50 percent. Fig. 15-a shows the variation of precipitation values ranging from zero mm to 1.25 mm, demonstrating a profound influence on the median reliability time in the Kiruna region. This change corresponds to a considerable reduction from 8754 hours to 3506 hours, representing a substantial decline of approximately 60 %.

In addition, the trendline for the data in Fig. 15-b reveals an exponential equation that describes the relationship between the MTBF and the variation in precipitation values. The exponential equations capture the nonlinear nature of this relationship, indicating that even slight variations in precipitation value can significantly impact MTBF, consequently leading to an increase in the frequency of failures. Therefore, it is necessary to take appropriate measures to mitigate the potential consequences of these changes. Moreover, the variation of precipitation from zero mm to 1.25 mm can change the MTBF from 9538 hours to 3505 hours, leading to a 63 % reduction in MTBF. This means this variation can significantly increase the number of failures and the assets need to be more resilient against such effective covariates.

Table 7
A sample of failure data associated with covariates for S&C with Object ID = 1.

ID	Start[a]	Stop[a]	Status[b]	Climate_id[c]	X1 (°C)	X2 (%)	X3 (mm)	X4 (m/s)	TBF*
1	0	15,891	1.00	1.00	–6.52	92	0.03	2.54	15,891
1	15,891	19,137	1.00	1.00	–0.12	85	0.01	5.25	3246
1	19,137	19,911	1.00	0.00	0.08	78	0.00	1.79	774
1	97,046	97,798	1.00	1.00	–10.25	77	0.00	6.88	752
1	97,798	98,846	1.00	0.00	–0.83	90	0.16	5.29	1048
1	98,846	99,431	1.00	1.00	–2.13	87	0.26	4.75	585
1	157,502	157,509	1.00	1.00	–5.00	89	0.00	5.71	7
1	157,502	157,509	0.00	0.00	–5.00	89	0.00	5.71	7

[a] Normal operation, unit is in hour,
[b] variable indicates the occurrence of failure or censorship (0 = censor),
[c] 1=Climate_based failure, 0= non-climatic-based failures

Table 8
Determining effective covariates on Cox PHM.

Region	Step	Covariate	Coef.(β_i)	Robust Std. Err.	p-value	95 % Conf. Interval
Kiruna	1	X_1	–0.001	0.002	0.58	–0.004 0.002
		X_2	–0.024	0.010	0.02	–0.043 –0.004
		X_3	1.122	0.778	0.15	–0.403 2.646
		X_4	0.000	0.013	0.96	–0.024 0.025
Kiruna	2	X_2	–0.023	0.011	0.03	–0.045 –0.001
		X_3	1.118	0.785	0.15	–0.421 2.657
Boden	1	X_1	–0.001	0.014	0.95	–0.028 0.026
		X_2	–0.001	0.010	0.56	–0.024 0.013
		X_3	–0.423	0.621	0.46	–1.639 0.793
		X_4	–0.021	0.052	0.69	–0.123 0.081
Borlänge	1	X_1	–0.010	0.007	0.17	–0.024 0.004
		X_2	–0.006	0.003	0.03	–0.010 –0.001
		X_3	0.139	0.137	0.31	–0.129 0.407
		X_4	0.146	0.041	0.00	0.066 0.225
Borlänge	2	X_2	–0.003	0.003	0.35	–0.010 0.000
		X_4	0.151	0.041	0.00	0.070 0.231
Borlänge	3	X_4	0.149	0.042	0.00	0.066 0.232
Gothenburg	1	X_1	–0.010	0.004	0.02	–0.019 –0.001
		X_2	0.005	0.003	0.11	–0.001 0.011
		X_3	–0.085	0.226	0.71	–0.529 0.358
		X_4	–0.018	0.026	0.50	–0.069 0.034
Gothenburg	2	X_1	–0.010	0.004	0.01	–0.019 –0.002
		X_2	0.005	0.003	0.13	–0.001 0.010

Table 9
Schoenfeld test result of assessing Cox proportional hazards assumption.

Region	Covariate	Chi2	df	p-value
Kiruna	X_2	1.40	1	0.23
	X_3	1.75	1	0.19
	Global test	2.86	2	0.24
Borlänge	X_4	2.63	1	0.11
	Global test	2.63	1	0.11

Table 10
Hazard rate equations for different failure modes according to Cox PH model.

Region	Hazard rate formula
Kiruna	$h_0(t, \mathbf{X}) = \frac{1.62}{14120} * \left(\frac{t}{14120}\right)^{0.62} * \exp(-0.023*X2 + 1.118*X3)$
	$h_1(t, \mathbf{X}) = \frac{1.52}{11136} * \left(\frac{t}{11136}\right)^{0.52} * \exp(-0.023*X2 + 1.118*X3)$
Boden	$h_0(t, \mathbf{X}) = \frac{1.44}{16705} * \left(\frac{t}{16705}\right)^{0.44}$
	$h_1(t, \mathbf{X}) = \frac{2.02}{40784} * \left(\frac{t}{40784}\right)^{1.02}$
Borlänge	$h_0(t, \mathbf{X}) = \frac{1.39}{9558} * \left(\frac{t}{9558}\right)^{0.39} * \exp(0.149*X4)$
	$h_1(t, \mathbf{X}) = \frac{1.43}{24529} * \left(\frac{t}{24529}\right)^{0.43} * \exp(0.149*X4)$
Gothenburg	$h_0(t, \mathbf{X}) = \frac{1.74}{12020} * \left(\frac{t}{12020}\right)^{0.74} * \exp(-0.010*X1 + 0.005*X2)$
	$h_1(t, \mathbf{X}) = \frac{1.27}{11618} * \left(\frac{t}{11618}\right)^{0.27} * \exp(-0.010*X1 + 0.005*X2)$

4.6. Climate adaptation actions

Traditionally, indicators like geometric and structural deterioration have been the primary focus of O&M planning. However, the results presented here reveal the necessity of incorporating additional variables, particularly meteorological specifications and climate change factors, into the design and O&M planning process. By considering meteorological factors alongside traditional indicators, managers can enhance their planning strategies' overall effectiveness and adaptability, ensuring the long-term sustainability and functionality of critical infrastructure assets under changing climatic conditions.

Our results show that infrastructure managers should adapt their design and O&M strategies to climate change to maintain the railway network's functionality, especially in sensitive parts like Kiruna railway station assets, which provide the majority of iron ore in Europe. Since S&Cs are selected as critical assets in this study, the following strategies can be proposed as climate adaptation planning.

First, preventive actions such as installing sensitive heaters to variations of weather conditions and accordingly increasing the number of inspections,

Second, protect the assets which are endangered by climate change, such as severe precipitation, can be covered by galleries or by other protectors,

Third, several design and construction regulations need to be reviewed to fulfill climate change demands. For instance, future precipitation in Sweden is projected to increase, which may impact the

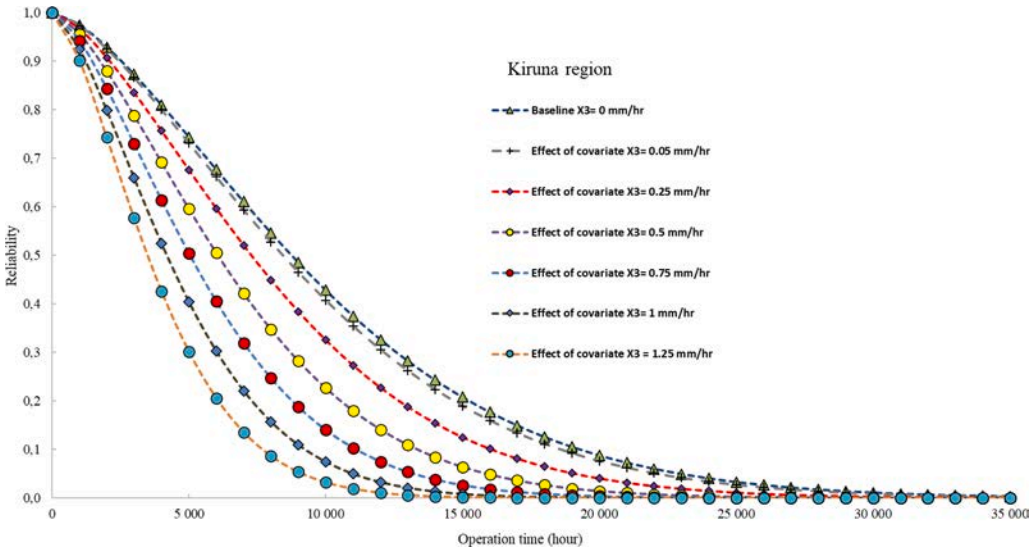

Fig. 14. The impact of varying precipitation values on the reliability over operation time for Kiruna region using the stratified Cox PH model for climate-related failure mode.

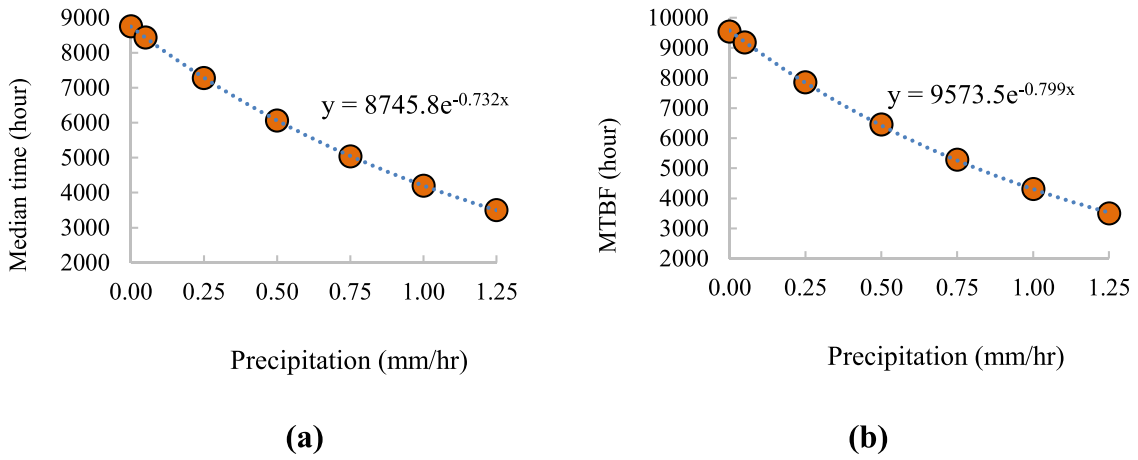

Fig. 15. Estimated exponential regression model between median time of reliability (a) and MTBF (b) and precipitation covariate for Kiruna region.

number of floodings in the urban railway assets. On the other hand, the current drainage system was designed according to the past criteria, which could not manage the volume and intensity of water in railway infrastructure. Therefore, modification of drainage systems at railway stations and renovation of culverts are other strategies that can mitigate the adverse effects of severe precipitation in the future.

5. Conclusion

This study investigates the impact of climate change on urban railway infrastructure, particularly focusing on switches and crossings (S&Cs) in the Swedish railway network. Climate-related events, such as extreme weather conditions, temperature variations, and severe precipitation, have been identified as significant challenges for railway systems, leading to reduced availability, safety concerns, decreased punctuality, and increased O&M costs. Since climate impact and its consequences are highly dependent on geographical features, it is required to categorize the railway network into different climate zones, which preserve climate homogeneity within each group. To achieve this, a representative sample of 40 stations chosen from various regions and machine learning/ K-means algorithm has been utilized to fulfill the aim. These stations clustered into four distinct climate zones based on their shared meteorological characteristics and climatic properties.

A reliability analysis using the Cox PHM is proposed to understand the railway system's behavior under changing climatic conditions. This model allows for integrating meteorological parameters and operational factors to predict the variability of climatic parameters and their impacts on urban railway infrastructure assets.

The proposed methodology has been validated by selecting a number of S&Cs, which are located in different railway stations in various climate zones. The study explored various databases to identify climate-related risk of S&C assets by developing climate_id feature. Furthermore, significant meteorological covariates and their impacts have been assessed to understand better the dependency between asset health and meteorological parameters considering future extreme weather events.

Sensitivity analysis shown that changing the precipitation value from zero to 1.25 mm in Kiruna region can decrease the median time of reliability and MTBF about 60 percent. By understanding the significant meteorological parameters and vulnerable assets, targeted adaptation measures can be developed to improve the resilience of railway infrastructure.

Declaration of Competing Interest

The authors declare that they have no known competing financial interests or personal relationships that could have appeared to influence

the work reported in this paper.

Data availability

Based on the confidential agreement between research projects and Trafikverket, sensored data can be provided on request. In addition the codes are available on request.

Acknowledgements

Authors gratefully acknowledge the funding provided by Sweden's innovation agency, Vinnova, to the project titled "Adapting Urban Rail Infrastructure to Climate Change (AdaptUrbanRail)" (grant no. 2021-02456) and "Robust infrastructure – Adapting railway maintenance to climate change (CliMaint)" (grant no. 2019-03181)"; and Kempe foundation which providing Postdoctoral scholarship through (grant no. JCK-2215). The authors gratefully acknowledge the in-kind support and collaboration of Trafikverket, SMHI, WSP AB, InfraNord, and Luleå Railway Research Center (JVTC).

References

Abeysekera, W., & Sooriyarachchi, M. (2009). *Use of Schoenfeld's global test to test the proportional hazards assumption in the Cox proportional hazards model: an application to a clinical study*.

Barabadi, A., Barabady, J., & Markeset, T. (2014). Application of reliability models with covariates in spare part prediction and optimization–a case study. *Reliability Engineering & System Safety, 123*, 1–7.

Barabadi, A., Barabady, J., & Markeset, T. (2011). Maintainability analysis considering time-dependent and time-independent covariates. *Reliability Engineering & System Safety, 96*(1), 210–217.

Bendell, A., Wightman, D. W., & Walker, E. V. (1991). Applying proportional hazards modelling in reliability. *Reliability Engineering & System Safety, 34*(1), 35–53.

Bienvenido-Huertas, D., Rubio-Bellido, C., Marín-García, D., & Canivell, J. (2021). Influence of the Representative Concentration Pathways (RCP) scenarios on the bioclimatic design strategies of the built environment. *Sustainable Cities and Society, 72*, Article 103042.

Bubeck, P., Dillenardt, L., Alfieri, L., Feyen, L., Thieken Annegret, H., & Kellermann, P. (2019). Global warming to increase flood risk on European railways. *Climatic Change, 155*, 19–36.

Chan Steven, C., Kendon Elizabeth, J., Ségolène, B., Giorgia, F., Elizabeth, L., & Fowler Hayley, J. (2020). Europe-wide precipitation projections at convection permitting scale with the Unified Model. *Climate Dynamics, 55*, 409–428.

Chong, C., Ying, L., Shixuan, W., Xianfang, S., Carla, D. C.-G., & Titmus Scott, & Syntetos Aris A. (2020). Predictive maintenance using cox proportional hazard deep learning. *Advanced Engineering Informatics, 44*, Article 101054.

Cox, D. R. (1972). Regression models and life-tables. *Journal of the Royal Statistical Society: Series B (Methodological), 34*(2), 187–202.

Ferranti, E., Chapman, L., Lee, S., Jaroszweski, D., Lowe, C., McCulloch, S., & Quinn, A. (2018). The hottest J uly day on the railway network: insights and thoughts for the future. *Meteorological Applications, 25*(2), 195–208.

Forzieri, G., Bianchi, A., e Silva, F. B., Herrera, M. A. M., Leblois, A., Lavalle, C., Aerts, J. C., & Feyen, L. (2018). Escalating impacts of climate extremes on critical infrastructures in Europe. *Global Environmental Change, 48*, 97–107.

Gao, X., Barabady, J., & Markeset, T. (2010). An approach for prediction of petroleum production facility performance considering Arctic influence factors. *Reliability Engineering & System Safety, 95*(8), 837–846.

Garmabaki, A. (2019). *Adapting railway maintenance to climate change (CliMaint) - Grant no. 2019-03181 [Grant]*. www.ltu.se/climaint.

Garmabaki, A., Ahmadi, A., Block, J., Pham, H., & Kumar, U. (2016). A reliability decision framework for multiple repairable units. *Reliability Engineering & System Safety, 150*, 78–88.

Garmabaki, A., Odelius, J., Thaduri, A., Famurewa, S. M., Kumar, U., Strandberg, G., & Barabady, J. (2022). *Climate change impact assessment on railway maintenance*. https://www.rpsonline.com.sg/proceedings/esrel2022/html/toc.html.

Garmabaki, A., Thaduri, A., Famurewa, S., & Kumar, U. (2021). Adapting railway maintenance to climate change. *Sustainability, 13*(24), 13856.

German Development Cooperation. (2009). *Adapting urban transport to climate change module 5f sustainable transport: A sourcebook for policy-makers in developing cities*. http://www.sutp.org.

Ghodrati, B. (2005). *Reliability and operating environment based spare parts planning*. Luleå tekniska universitet.].

Guido, R., Alfredo, R., Luca, P., & Paola, M. (2020). Assessing future variations in landslide occurrence due to climate changes: insights from an Italian test case. In *Geotechnical Research for Land Protection and Development: Proceedings of CNRIG 2019* (p. 7).

IPCC. (2014). *Climate Change: Impacts, Adaptation, and Vulnerability Working Group II Contribution to the Fifth Assessment Report of the Intergovernmental Panel on Climate Change*.

IPCC. (2022). Climate change 2022: Impacts, adaptation, and vulnerability. In *Contribution of Working Group II to the Sixth Assessment Report of the Intergovernmental Panel on Climate Change*.

Jenkins, K., Gilbey, M., Hall, J., Glenis, V., & Kilsby, C. (2014). Implications of climate change for thermal discomfort on underground railways. *Transportation Research Part D: Transport and Environment, 30*, 1–9.

Kleinbaum, D. G., & Klein, M. (1996). *Survival analysis a self-learning text*. Springer.

Kumar, S., & Banerji, H. (2022). Bayesian network modeling for economic-socio-cultural sustainability of neighborhood-level urban communities: Reflections from Kolkata, an Indian megacity. *Sustainable Cities and Society, 78*, Article 103632.

Liu, B., Liang, Z., Parlikad, A. K., Xie, M., & Kuo, W. (2020). Condition-based maintenance for systems with aging and cumulative damage based on proportional hazards model. *Value Based and Intelligent Asset Management: Mastering the Asset Management Transformation in Industrial Plants and Infrastructures*, 211–231.

Louit, D. M., Pascual, R., & Jardine, A. K. (2009). A practical procedure for the selection of time-to-failure models based on the assessment of trends in maintenance data. *Reliability Engineering & System Safety, 94*(10), 1618–1628.

Miller, R., & Huntsinger, L. (2023). Climate change impacts on North Carolina Roadway System in 2050: A systemic perspective on risk interactions and failure propagation. *Sustainable Cities and Society*, Article 104822.

Moreau, T., O'quigley, J., & Lellouch, J. (1986). On D. Schoenfeld's approach for testing the proportional hazards assumption. *Biometrika, 73*(2), 513–515.

Nilsen, I. B., Hanssen-Bauer, I., Tveito, O. E., & Wong, W. K. (2021). Projected changes in days with zero-crossings for Norway. *International Journal of Climatology, 41*(4), 2173–2188.

Nissen, A. (2009). *Development of life cycle cost model and analyses for railway switches and crossings*. Lulea university of technology.].

Palin, E. J., Thornton, H. E., Mathison, C. T., McCarthy, R. E., Clark, R. T., & Dora, J. (2013). Future projections of temperature-related climate change impacts on the railway network of Great Britain. *Climatic Change, 120*, 71–93.

Pour, S. H., Abd Wahab, A. K., Shahid, S., Asaduzzaman, M., & Dewan, A. (2020). Low impact development techniques to mitigate the impacts of climate-change-induced urban floods: Current trends, issues and challenges. *Sustainable Cities and Society, 62*, Article 102373.

Rausand, M. B., Anne, & Hoyland, A. (2020). *System Reliability Theory: Models, Statistical Methods, and Applications*. John Wiley & Sons, Inc. https://doi.org/10.1002/9781119373940

Rianna, G., Reder, A., Pagano, L., & Mercogliano, P. Assessing future variations in landslide occurrence due to climate changes: Insights.

Salimi, M., & Al-Ghamdi, S. G. (2020). Climate change impacts on critical urban infrastructure and urban resiliency strategies for the Middle East. *Sustainable Cities and Society, 54*, Article 101948.

Sarkar, K., Chowdhury, R., & Dasgupta, A. (2017). Analysis of survival data: challenges and algorithm-based model selection. *Journal of Clinical and Diagnostic Research: JCDR, 11*(6), LC14.

Schlögl, M., & Matulla, C. (2018). Potential future exposure of European land transport infrastructure to rainfall-induced landslides throughout the 21st century. *Natural Hazards and Earth System Sciences, 18*(4), 1121–1132.

Schoenfeld, D. (1980). Chi-squared goodness-of-fit tests for the proportional hazards regression model. *Biometrika, 67*(1), 145–153.

Si, X.-S., Wang, W., Hu, C.-H., & Zhou, D.-H. (2011). Remaining useful life estimation–a review on the statistical data driven approaches. *European journal of operational research, 213*(1), 1–14.

SMHI. *Swedish National Knowledge Centre for climate change adaptation*. https://www.smhi.se/en/theme/climate-centre.

SMHI. (2015). *Climate indicator - Extreme precipitation*. https://www.smhi.se/en/climate/climate-indicators/climate-indicators-extreme-precipitation-1.91474.

Thaduri, A., Famurewa, S., Garmabaki, A., & Kumar, U. (2021). Adapting railway maintenance to climate change. *Sustainability, 13*(24), 1–27.

Thijssens, O., & Verhagen, W. J. (2020). Application of extended cox regression model to time-on-wing data of aircraft repairables. *Reliability Engineering & System Safety, 204*, Article 107136.

Tyler, K. (2015). Sea level rise adaptation primer: a toolkit to build adaptive capacity on Canada's Coasts. *Presentation. Climate Action Secretariat, BC Ministry of Environment: Prince George*. Prince George: BC Ministry of Environment.

Vogel, M. M., Zscheischler, J., Wartenburger, R., Dee, D., & Seneviratne, S. I. (2019). Concurrent 2018 hot extremes across Northern Hemisphere due to human-induced climate change. *Earth's future, 7*(7), 692–703.

World bank group. (2021). Climate Change Knowledge Portal. https://climateknowledgeportal.worldbank.org/country/sweden/cmip5.

Yakubovich, A., & Yakubovich, I. (2018). Analysis of the multidimensional impact of climate change on the operation safety of the road network of the permafrost zone of Russia. *Intelligence Innovation Investment, 3*, 77–83.

Zheng, H., Kong, X., Xu, H., & Yang, J. (2021). Reliability analysis of products based on proportional hazard model with degradation trend and environmental factor. *Reliability Engineering & System Safety, 216*, Article 107964.